AGU PUBLICATIONS

JGR

Journal of Geophysical Research: Space Physics

RESEARCH ARTICLE

10.1002/2013JA018926

This article is a companion to *Dorville et al.* [2014] doi:10.1002/2013JA018927.

Key Points:
- The method enables to find the normal to a 1-D layer and a normal coordinate
- The method is applicable to magnetopause data analysis
- Spatial profiles of all plasma parameters and fields can be obtained

Correspondence to:
N. Dorville,
nicolas.dorville@lpp.polytechnique.fr

Citation:
Dorville, N., G. Belmont, L. Rezeau, N. Aunai, and A. Retinò (2014), BV technique for investigating 1-D interfaces, *J. Geophys. Res. Space Physics*, *119*, 1709–1720, doi:10.1002/2013JA018926.

Received 5 APR 2013
Accepted 26 JAN 2014
Accepted article online 3 FEB 2014
Published online 7 MAR 2014

BV technique for investigating 1-D interfaces

Nicolas Dorville[1], Gérard Belmont[1], Laurence Rezeau[1], Nicolas Aunai[2], and Alessandro Retinò[1]

[1]LPP, Ecole Polytechnique, CNRS, UPMC, Université Paris Sud, Palaiseau, France, [2]Institut de Recherche en Astrophysique et Planétologie, Université de Toulouse, CNRS UMR5277, Toulouse, France

Abstract To investigate the internal structure of the magnetopause with spacecraft data, it is crucial to be able to determine its normal direction and to convert the measured time series into spatial profiles. We propose here a new single-spacecraft method, called the BV method, to reach these two objectives. Its name indicates that the method uses a combination of the magnetic field (B) and velocity (V) data. The method is tested on simulation and on Cluster data, and a short overview of the possible products is given. We discuss its assumptions and show that it can bring a valuable improvement with respect to previous methods.

1. Introduction

The Earth magnetopause is the outer boundary of the terrestrial magnetosphere. Outside of the dayside magnetopause boundary, the magnetosheath plasma is the shocked solar wind plasma, i.e., cold and dense, with a magnetic field direction essentially determined by the solar wind one. Inside of it, the magnetospheric plasma is comparatively hot and tenuous, with a magnetic field direction essentially determined by the planetary one. Experimentally, investigating the magnetopause structure by spacecraft measurements is made difficult by the fact that the boundary is not steady: it can be shaken by the variations of the solar wind pressure and perturbed by different kinds of waves, incident body waves and surface waves. It can also be locally and temporarily the place of different surface instabilities, implying or not magnetic reconnection, such as Kelvin-Helmholtz, Rayleigh-Taylor, or tearing instabilities [*Hasegawa*, 2012].

Two pieces of information are crucial to investigate the magnetopause nature:

1. Accurately determine the normal direction of the current sheet : a good precision on the normal magnetic field component B_n is very important to understand the nature of the layer. In a strictly planar and stationary configuration, $B_n = 0$ or not leads to different types of magnetohydrodynamics discontinuities, even if the nonnull B_n is very small.
2. Determine an approximate spatial coordinate along the normal, to be able to draw the spatial profiles of the different relevant parameters, in the boundary frame, i.e., independently of the velocity at which these profiles are traversed by the spacecraft.

Several methods have been developed for both of these two purposes.

To study the large-scale shape of the boundary, its motion and its orientation, multispacecraft methods have been developed, particularly for the European Space Agency (ESA) Cluster mission [see *Paschmann and Daly*, 1998; *Paschmann and Sonnerup*, 2008; *Dunlop et al.*, 2002a, 2002b]. These methods are essentially based on timing differences between spacecraft and all rely on strong assumptions on the boundary: its form (plane or slightly curved at the scale of the spacecraft tetrahedron), its stationarity (constant profile and width, hereafter CTA for "Constant Thickness Approach" [*Haaland et al.*, 2004]), or its velocity with respect to the spacecraft (hereafter CVA for "Constant Velocity Approach" [*Russell et al.*, 1983]). Others are "single-spacecraft" methods: they also rely on assumptions on the boundary properties such as planarity and stationarity, but they use in addition theoretical knowledge on the measured physical quantities, such as conservation laws. When using in particular the magnetic field data, the MVAB (minimum variance analysis on the magnetic field $\mathbf{B}$) method [*Sonnerup and Scheible*, 1998] takes advantage that $\mathrm{div}(\mathbf{B}) = 0$, which draws $B_n = \mathrm{cst}$ in the 1-D case. Its variant MVABC (C for corrected) adds the constraint $B_n = 0$, using the additional information that the magnetopause normal component B_n is null for closed magnetopause and is always much smaller than the other components, even in the case of an open magnetopause. This allows to handle cases when two components are nearly constant and not a single one (i.e., when two eigenvalues of the variance-covariance matrix are small). The normal direction can also be determined as the direction of

maximum variance of the electric field, possibly determined by $\vec{E} = -\vec{V} \otimes \vec{B}$. This method does not assume $B_n = 0$, but it can hardly be expected either to provide a sufficient accuracy to determine a reliable B_n, in general (the usual values of B_n being less than 10 nT).

When the magnetopause can be assumed 1-D and stationary but when its thickness is small compared to the local thermal ρ_i, making the kinetic effects nonnegligible with respect to the MHD ones, the experimental profiles have to be compared with kinetic models. If the layer is tangential, such models can be found in the literature (see *De Keyser and Roth* [1998] for a review of the first models of this kind and *Belmont et al.* [2012] for the most recent one). The experimental method developed in this paper should enable to perform such comparisons. When the magnetopause layer cannot be assumed 1-D, like in the case of reconnection events, other methods are needed. *Mozer and Retinò* [2007] explains how to estimate the normal magnetic field and tangential electric field in these cases. Some methods have been developed to reconstruct the magnetopause structure, assuming it is 2-D and stationary and that it is governed by MHD equations: these are the Grad-Shafranov reconstruction methods (see *Hasegawa et al.* [2004] for a long-duration reconstruction). A review and discussion of short- and long- duration methods is made in *De Keyser* [2006]. Experimentally, it is often difficult to decide whether the 1-D or the stationarity hypothesis has to be questioned first. Future comparison between the results of the reconstruction methods and those of the method proposed in this paper should be interesting in this respect.

To find an approximate normal coordinate allowing to investigate the internal structure of the layer and to determine profiles across it, other methods have been developed independently, introducing the notion of "transition parameter" [*Lockwood and Hapgood*, 1997]. These methods can be used with single-spacecraft data. They also rely on assumed magnetopause properties, and they have been based hitherto on the variations in density and temperature of the electron population. This of course limits the temporal resolution of the method—and consequently its spatial one—to the resolution of the electron experiment.

We propose here a new "single-spacecraft" method, referred to hereafter as "BV" to show that the magnetic field and the flow velocity data are used simultaneously, to analyze dayside magnetopause-like interfaces. It combines the two types of methods previously described in such a way that it allows to determine in the same operation the magnetopause normal with an expectingly improved accuracy *Dorville et al.* [2014] where this improvement is shown to allow a better mass flux conservation on a particular case) and a transition parameter expectingly closer to a real spatial coordinate. Fitting the magnetic field hodogram with a prescribed form, which is here an elliptical arc, allows to determine the normal direction with a fairly good accuracy. In addition, the angle α characterizing the position on the elliptical arc provides a reliable transition parameter inside the current layer, which can be viewed as a proxy for a normalized coordinate in the normal direction. On the other hand, as soon as the normal direction is known, the velocity measurements give a nonnormalized normal coordinate, which is just the integral of the normal flow velocity u_n. It can give, in particular, a fairly good estimate of the physical width of the layer whenever the measured velocity should be in most cases dominated by the motion of the boundary. Using simultaneously the magnetic and velocity measurements just consists in imposing that the normal coordinate determined by only the velocity measurements is proportional to the transition parameter coming only from the magnetic measurements. Since u_t is generally larger with larger variations than u_n (for typical values see *Soucek and Escoubet* [2012]), the integral of u_n is very sensitive to the normal direction. This enables to improve the determination of this direction with respect to the magnetic determination alone. It is to be noted however that all the available magnetic data are used, with their high time resolution, even if the particle data that allow improving the result are known with a much lower time resolution.

Section 2 presents the principles of the BV technique, and section 3 presents the different validation tests performed. The method allows to draw spatial profiles of any physical parameter across the magnetopause boundary. Examples of such profiles are presented in section 4, before discussing the interest and the limitations of the BV method and concluding in section 5.

2. Principles of the Method

As the previous equivalent methods, the basic assumption of the BV technique is that apart from oscillating perturbations, the boundary is sufficiently one-dimensional and stationary at the scale of the spacecraft crossing. To explain the principles of this method, we use here a set of Cluster data on 3 March 2008,

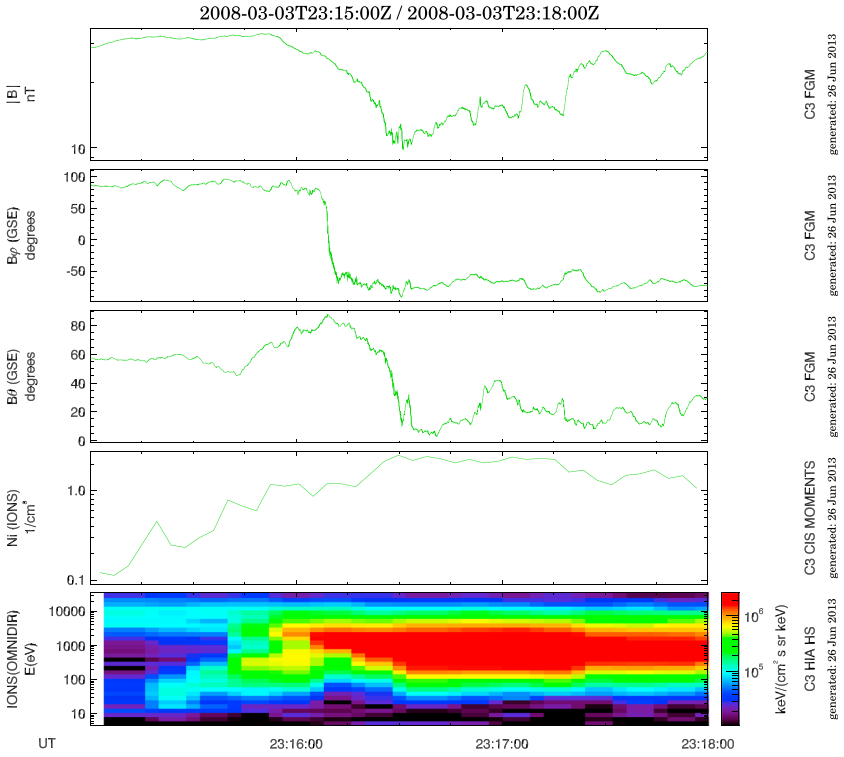

Figure 1. Density, energy spectrogram, and magnetic field observed by Cluster C1 around 23 h 16 min on 3 March 2008. The jump of density, change in plasma energy composition, and rotation of magnetic field show that the satellite is crossing the magnetopause.

when Cluster C3 encounters the magnetopause around 23:16 UT at the position (in Earth radii) (13.6, 3.7, −0.7) in the GSE coordinate system (the input interval for BV is 23:15.15–23:16.45, then a time interval will be selected by the method). As it can be seen in Figure 1, the transition in the energy spectrogram of the plasma, the density gradient, and the rotation of magnetic field confirm the crossing of the magnetopause. For some figures, we will also use another crossing of the magnetopause, when C3 encounters the boundary on 1 April 2008 around 10h12 UT (input interval used: 10:11.40–10:13.40 UT). The method uses principally the magnetic field data [*Balogh et al.*, 1997]. In section 2.1 we describe how we obtain an initial guess of the normal direction with only the magnetic field data. Section 2.2 then explains the BV method itself, which combines magnetic field and ion velocity data [*Rème et al.*, 1997]. A global algorithmic viewpoint on the BV method, summarizing both sections is given in Figure 4.

2.1. Initialization With Only the Magnetic Field Data

In order to correctly initialize the minimization process of the complete BV method, involving magnetic field and ion velocity data, it is necessary to perform first an initialization stage, which provides an approximate frame and a first elliptical fit. This stage uses only the magnetic field data. It is done itself in several steps. The first step consists in finding a first approximation of the normal direction via a MVABC technique [*Sonnerup and Scheible*, 1998]. Figure 2 shows the tangential hodogram derived by this method. In this example as in many other observations [*Panov et al.*, 2011], we observe a C-shaped hodogram, which can be fitted by an elliptical model. Although the general concept of the BV method is valid for any 1-D layer, its present implementation is conceived for such kind of hodograms. Further generalization to more complicated hodograms (in particular for the S-shaped hodograms described in *Panov et al.* [2011]) will be a subject of future work. The second step consists in selecting the "magnetic ramp," i.e., the interval of data where the gradient of B_L (defined as the component of the magnetic field in the maximum variance direction) is precisely located. Here the time interval calculated is 23:15.53–23:16.34 UT. We then further automatically select the data points by choosing only a sample of "representative points" among them. This step has a double purpose: eliminate the perturbations that can be considered as "noise," and make the different parts of the crossing equally represented in the statistics, even if the spacecraft does not spend the same time in these different

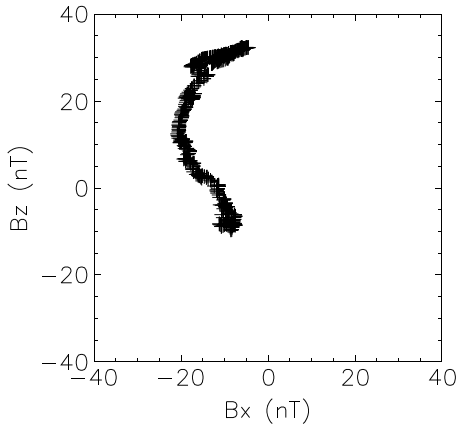

Figure 2. Hodogram of the magnetic field in the tangential MVABC plane for the Cluster C3 magnetopause crossing of 3 March 2008.

parts. First, we roughly eliminate the perturbations by discarding all points too far from the mean trajectory of the hodogram, and we represent each too close packet of points by only one single point. An elliptic fit and a new reference coordinate system are derived from these points, using a Powell minimization algorithm [*Powell*, 1964]. This part is summarized in the first step of Figure 4. The points selected in this way and the corresponding fit in the new frame are shown in Figure 3. The hodogram of Figure 3 appears turned by about $\frac{\pi}{2}$ from Figure 2. This is unimportant since only the normal direction is physically relevant, and the two tangential components are equivalent for this study. Figure 2 has the *M* component of the MVABC method as *x* axis, while Figure 3 has not. Then, the second goal is achieved by slicing the angles α domain on the ellipse in a number of intervals and keeping a constant number of points in each α slice, in agreement with the hypothesis (to be justified in next section) that α varies linearly with y, the function $y(t)$ being the integral of the normal velocity u_n. Using this initialization, we proceed to a new elliptic fit, which provides a fine initialization for the BV method itself. The second step of Figure 4 summarizes this part of the initialization. Note that this point selection is only used to help to the initialization and that all the data will be used for the next step of the algorithm.

2.2. Simultaneous Use of Magnetic and Velocity Data

The above stage has given an initial guess for the BV method regarding (1) the normal direction and (2) the parameters describing the elliptic hodogram. The main part of the method then consists in using the temporal information $\mathbf{B}(t)$, together with the velocity measurements from the hot ion analyzer (HIA) experiment (cf. *Rème et al.*, 1997). This last part of the process is summarized on step 3 in Figure 4. Going back to the totality of the $\mathbf{B}$ data points, one minimizes the distance between them and the elliptical model $\mathbf{B}(y)$. The integration providing the parameter y could be done with the original spin resolution of the velocity data. It is done here through an interpolation at the magnetic field time resolution in order to make the curve smoother (this has no other noticeable influence on the result). For this step we assume that this normal velocity is dominated by the layer velocity, i.e., that the normal velocity within the frame of the layer is sufficiently smaller. This is directly true for a tangential discontinuity but is a stronger hypothesis when the normal magnetic field is nonnull. Let us show that in most circumstances, this approximation should not bring a strong inaccuracy in the normal determination.

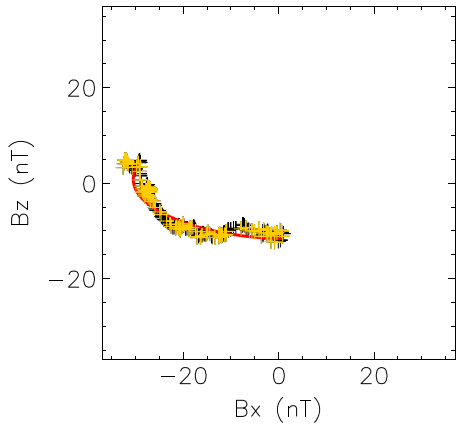

Figure 3. Initialization fit of the hodogram in initialization frame for the Cluster C3 magnetopause crossing of 3 March 2008. The data are in black, the selected points in yellow, and the initialization fit in red.

1. If the density is constant and the Walén test fulfilled, that is, in the case of a rotational discontinuity, the flow in the frame of the boundary should be at normal Alfvén speed, possibly nonnegligible when B_n is large. However, in this case, the profile of V_n (constant Alfvén speed added to the time-varying velocity of the layer) should still be distinguishable from tangential velocities profiles (larger, with larger variations, and rotating with the field), which is sufficient to ensure that the BV algorithm provides a good determination of the normal. Regarding the determination of the transition parameter, the normal velocity can then be corrected to deduce a right position.

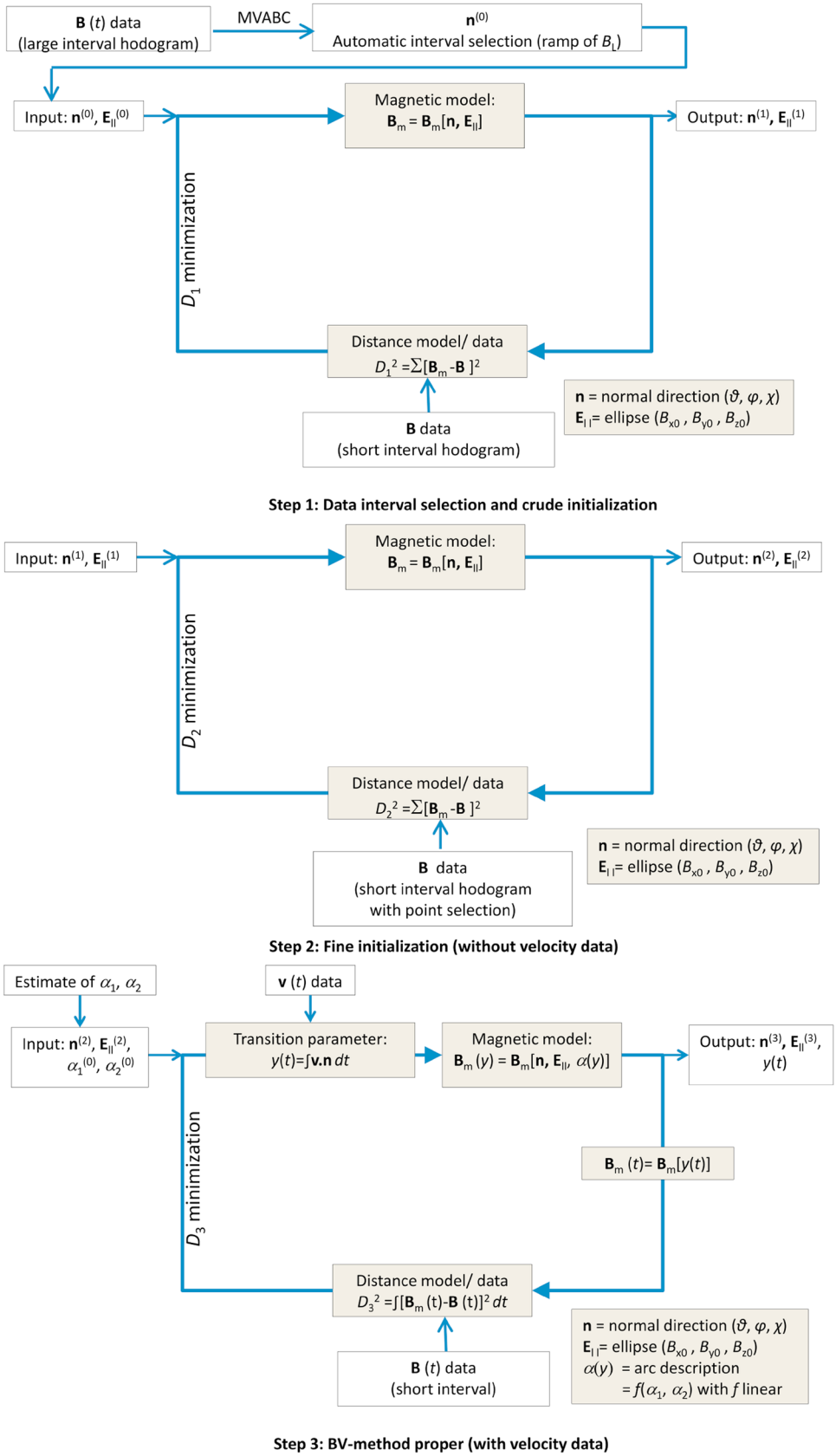

Figure 4. Algorithm used for initialization and BV method. E_{II} stands for the elliptical form that is determined at each step (characterized by B_{x0}, B_{y0}, and B_{z0}).

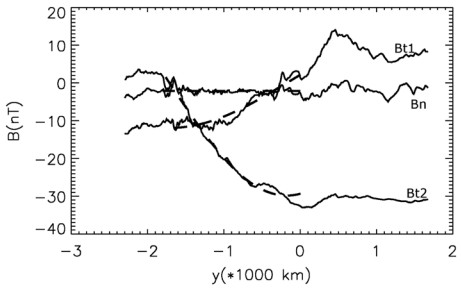

Figure 5. Fit (dashed) of the three components of the magnetic field (solid lines) along the normal coordinate for the Cluster C3 magnetopause crossing of 3 March 2008.

2. If the normal magnetic field is not null but the discontinuity is not rotational at all, the physics of the discontinuity may be quite different from the usual rotational discontinuity (no constant V_{An} speed). Nevertheless, the previous arguments concerning the contrast between normal and tangential components still hold and the study presented in the companion paper [*Dorville et al.*, 2014] shows furthermore that the velocity across the discontinuity can then be much smaller than V_{An}.

The minimization of the distance to temporal data is done with respect to the three angles that characterize the rotation of the ellipse proper frame and to the parameters of the elliptic hodogram, initialized previously, using the same Powell algorithm as above. The distance to be minimized is

$$\sum \sqrt{(B_{dx} - B_{mx})^2 + (B_{dy} - B_{my})^2 + (B_{dz} - B_{mz})^2} \tag{1}$$

where $\mathbf{B}_d$ represents the data points and $\mathbf{B}_m$ represents the model. This model is given by

$$B_{mx} = B_{x0} \cos \alpha \tag{2}$$

$$B_{my} = B_{y0} \tag{3}$$

$$B_{mz} = B_{z0} \sin \alpha \tag{4}$$

with

$$\alpha = \alpha_1 + (\alpha_2 - \alpha_1)\, y/y_{\max}, \tag{5}$$

y being the position deduced from the normal velocity integral. The magnetic field data and velocity data are turned in the good frame by a rotation of $M(\theta, \phi, \chi)$. The parameters of the fit are θ, ϕ, and χ (three angles that define the rotation matrix), B_{x0}, B_{y0}, B_{z0}, α_1, and α_2 (the five quantities needed to define the elliptic arc). Figure 4 summarizes the algorithm for initialization and proper BV method.

This final stage provides all the needed outputs: the normal direction, the spatial position $y(t)$ along this normal, and the fit of magnetic field, as illustrated, for example, in Figure 5. Note that the method provides the position directly in physical units (namely in kilometers here) and not only a normalized transition parameter. This allows in particular to get an estimate of the magnetopause thickness. Here the computed magnetopause thickness is 1800 km, and the linear Pearson correlation coefficients of the fit of B_x and B_z are 0.99 and 0.95. The spatial position is determined only inside the rotation layer. The method does not provide any information outside. If necessary, the spatial position y can be extrapolated linearly outside the boundary, in order to plot approximate profiles of any plasma parameter on scales larger than the ramp region and so provide some insight into the context.

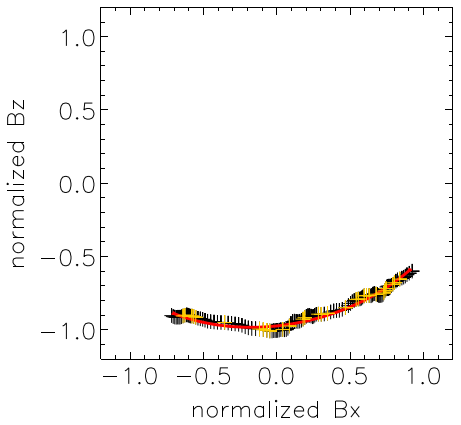

Figure 6. Fit of the hodogram of the magnetic field in the simulation for a virtual satellite crossing far from X point in the numerical simulation. The data are in black, the selected points in yellow, and the fit in red.

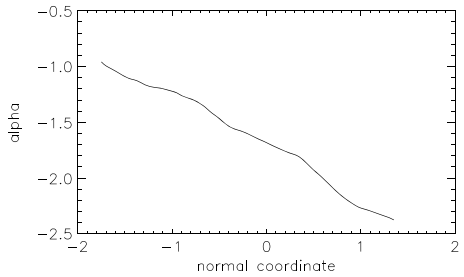

Figure 7. Angular position in radians on the ellipse along the normal direction in the simulation for a virtual satellite crossing far from *X* point.

3. Validations of the Method

Having presented how the BV method works in the previous section, we will now explain what led us to this way of proceeding and what are the different validation tests we have performed. We will discuss first the validity and the limitations of the hypotheses and discuss afterward the consistency of the obtained results. We used three different tools to develop and validate the method: a simple code to generate artificial magnetic field data (3.2.1), a simulation of an asymmetric reconnection layer with a hybrid code (3.2.2) [*Aunai et al.*, 2013], and real data from the Cluster mission (3.2.3), coming from a 2008 low-latitude magnetopause crossings list compiled by N. Cornilleau-Wehrlin.

3.1. Hypotheses: Elliptical Shape and Linear Angular Velocity

The first new assumption of the method, with respect to previous single-spacecraft data analysis methods, is the elliptic shape of the tangential magnetic field hodogram, the simplest model geometry to describe C-shaped hodograms. This elliptical shape is indeed consistent with a simple generalization of the circular model $\mathbf{B}(y)$ proposed by *Panov et al.* [2011]

$$\frac{B_L}{B_{L0}} = \tanh(y/L) \tag{6}$$

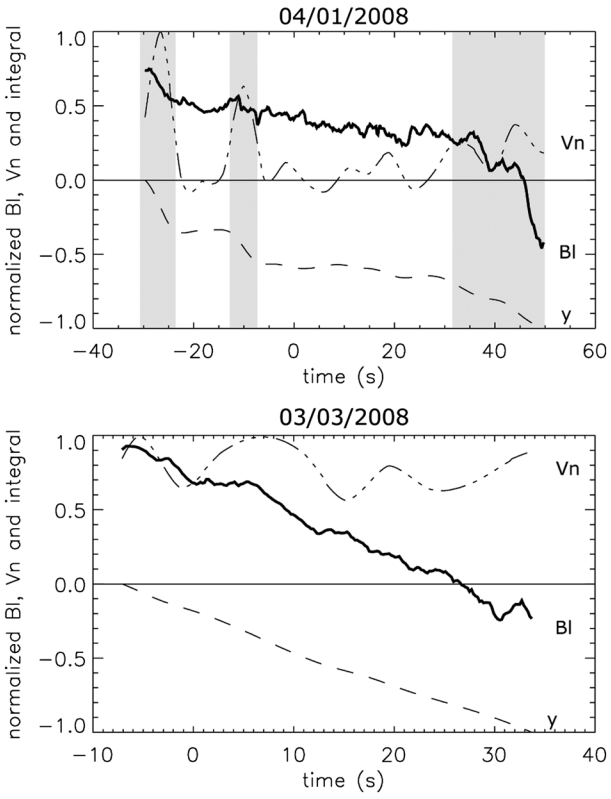

Figure 8. Normalized B_L (plain), V_n (dash dotted), and y (dash) for two 2008 magnetopause crossings. For 3 March y is normalized to 1804 km, V_n to 56 km/s, and the magnetic field to 31 nT. For 1 April the normalization values are, respectively, 533 km and 41 km/s and also 31 nT. One can see that the higher values of v_n (shaded areas) are correlated with the stronger gradients in B_L.

$$\frac{B_M}{B_{M0}} = \frac{1}{\cosh(y/L)} \tag{7}$$

These formulas imply in particular that $B_L^2/B_{L0}^2 + B_M^2/B_{M0}^2 = 1$, which has been used as a test of the elliptical shape.

The efficiency of the method can be tested first on a numerical simulation of reconnection, far from the *X* point. Its applicability is not obvious in this case, since before the development of the reconnection pattern, the initial condition is purely tangential, without any rotation. Nevertheless, the Hall effect creates a self-consistent out-of-plane magnetic component during the reconnection process. In the considered asymmetric configuration (asymmetric in density and temperature and coplanar and antisymmetric in magnetic field) this results in a C-shaped hodogram between the separatrices. Figure 6 shows the magnetic field in the interval that corresponds to the gradient of B_L. The error $\frac{\Delta B}{B}$ is here less than 2%. We have checked that this good accuracy is kept as long as the crossing considered is not too close to the *X* point, which is generally the case for crossings of the reconnected magnetopause, or to the limits of the simulation domain.

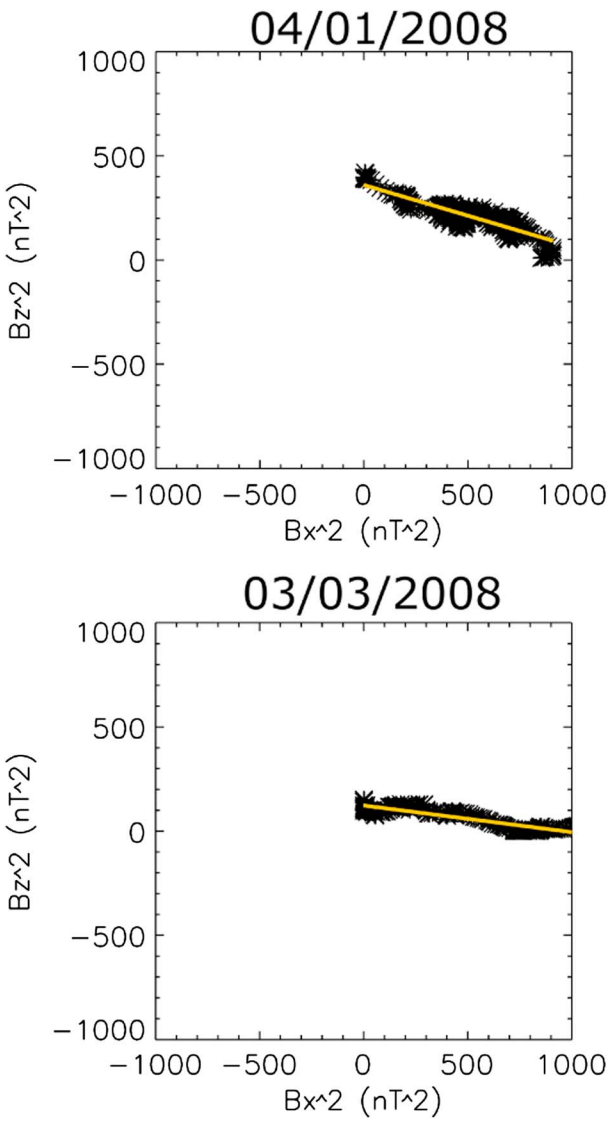

Figure 9. Hodogram of the square of the components of magnetic field in the tangential LM plane for two Cluster C3 magnetopause crossings of 1 April 2008 and 3 March 2008.

Regarding the analytical form of $\alpha(y)$ (see equation (5)), we also checked the validity of the linear hypothesis in the same simulation study. Figure 7 shows how α varies as a function of the normal coordinate y_s of the simulation. We observe that apart from weak periodic variations, the linear form is well satisfied. It is worth explaining that the weak periodic departures from the linear variations (which can be well described by the three of four first terms of a Fourier transform) can indeed be accounted for in the minimization procedure, but it would increase the number of free parameters and drastically affect the convergence of the minimization process.

Regarding Cluster data, Figure 8 shows temporal profiles of B_L and V_N and its integral y for two 2008 magnetopause crossings. For 3 March, the velocity appears to always stay in the same range and its integral and B_L vary quite uniformly. We see, on the contrary, for 1 April that the strong gradients of B_L appear to be correlated with the higher normal velocities, while slow velocities are correlated with periods of quite constant magnetic field. This is in good agreement with the hypothesis that the normal flow speed across the boundary remains small with respect to the speed of the boundary.

3.2. Consistency of the Results and Limitations

3.2.1. Artificial Data

Regarding the consistency of the results, the first test consists in running the first part of the method (identification of the ellipse and of its proper coordinate system) on a magnetic field that is artificially generated with an elliptic hodogram. Such artificial data have thus been constructed with the same analytical formulas as those of the program. Then this has been randomly rotated and added to a random Gaussian noise centered on the signal, with a relative amplitude up to 50%. The result is that the method always allows to find the good initial normal direction with at least five significant numbers and the right ellipse parameters, whenever the noise does not exceed 30%.

3.2.2. Simulation Data

The second test consists in using the above numerical simulation [*Aunai et al.*, 2013] to mimic a real magnetopause crossing. In order to make the method work, we must modify the simulation results in a way that makes it likely closer to most real magnetopause crossing: we multiply the tangential velocities by a large factor ($\approx$ 10). Thanks to this change, the tangential velocities get a much larger contrast than the normal ones, which is necessary for the program convergence. It must be noted that such a contrast of the tangential velocities is expected to exist most often at the magnetopause, except very close to the stagnation point at the magnetospheric nose. Everywhere else, the tangential velocity change is most generally observed to be of the order of a few 100 km/s, while the normal one (in the spacecraft frame) is generally about 5 or 10 times smaller, with a still smaller variation. In order to focus on the reconnection process without interference from any Kelvin-Helmholtz instability, the simulation did not include such a velocity shear.

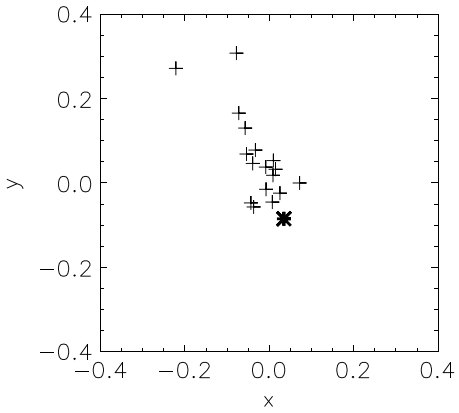

Figure 10. Several single-spacecraft and multispacecraft methods normal direction positions in the plane perpendicular to the MVABC mean normal for a benchmark case from *Haaland et al.* [2004]. The star represents the result of BV method. The distance from the origin in this plane corresponds to the sin θ, where θ is the angle from the mean normal direction.

Furthermore, the normal velocity of the virtual spacecraft considered with respect to the boundary has to be chosen large enough with respect to the normal velocities in the boundary frame. This is generally, as already mentioned, a reasonable hypothesis for a real magnetopause crossing.

Under these assumptions, we get normals with an angular precision oscillating between 0° and 5° for different virtual crossings (with the corresponding errors on the shape of the tangential hodogram) and 0–5% errors on the *y* parameter (and derivative), which corresponds to the internal velocity and the approximations on $\alpha(y)$.

The result is not changing as long as the virtual spacecraft crosses the simulation far enough (several d_i) from the *X* point, where the 2-D effects are not dominant. In these cases, the precision of the MVABC method is of the same order, (slightly better or worse, depending on the cases), because B_n is actually very close to 0. For a "true" normal direction of (0,1,0), we got for example (0.011, 0.999, 0.050) with BV, (−0.002, 0.987, 0.160) with MVABC, (−0.003, 0.559, 0.829)with MVAB, and (−0.005, 0.998, 0.057) with var(VxB). As MVAB is failing on this case, the three other methods are close to the good result, BV and var(VxB) being better than MVABC.

3.2.3. Cluster Data

Regarding real Cluster data, the measurements show more perturbations, but the variations of the field value around the mean ellipse are still around 5% for most C-shaped hodograms. A good test for the elliptical shape of the tangential hodogram is to plot $B_z^2(B_x^2)$, which must be linear for a tangential ellipse. Figure 9 shows this plot for two magnetopause crossings on 3 March 2008 and 1 April 2008. It shows that the elliptical shape is a good approximation.

It is clear, from the tests on the numerical simulation, that the BV method has limitations related to the necessary contrast between the normal and tangential component profiles. When applied to real Cluster data, these limitations may have, in some occasions, consequences on the results obtained. We will discuss these limitations in the conclusion section. It is to be noted however that these limitations are based on assumptions which are different—and generally weaker (see section 5)—than those of the other single-spacecraft methods such as MVAB or MVABC. We will present a detailed study on a case [*Dorville et al.*, 2014], where the BV method leads to a better understanding and more precise results than MVAB(C).

When all the methods are confidently applicable, the results seem to be consistent with each other and with the theoretical knowledge. We show in Figure 10 a reproduction of a figure from *Haaland et al.* [2004] corresponding to a benchmark case where different methods have been used. The center of the figure is the mean MVABC normal and other single-spacecraft and multispacecraft methods are represented in a polar plot in the plane perpendicular to this normal. The result of the BV method on C1 spacecraft is indicated by a star. The figure shows that the result is inside the dispersion range of the points. The thickness of the layer always stands between a few hundreds of kilometers and a few thousands, which is consistent with literature, the tangential velocities being generally 1 order of magnitude larger than the normal one (in the spacecraft frame). The normal magnetic fields always stand between 0 and 20 nT,

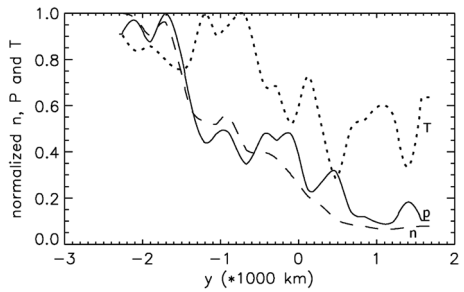

Figure 11. Evolution with normal position of normalized density (to 2.5 cm^{-3}), pressure (to 0.17 nPa), and temperature (to 6 MK) measured by Cluster C3 Cluster Ion Spectrometry instrument for the 3 March 2008 crossing.

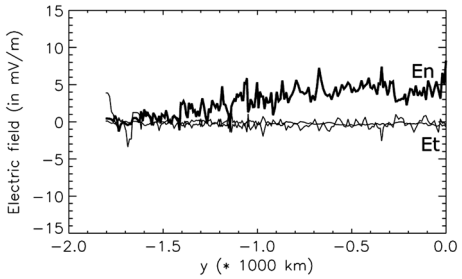

Figure 12. Evolution with normal position of the electric field measured by Cluster C3 EFW instrument for the 3 March 2008 crossing.

the nonnull values being reliable and quantitative indications of a connected boundary, which could hardly be obtained previously.

On two magnetopause crossings (15 April 2008 15h20 by C1 [*Dorville et al.*, 2014] and 3 March 2008 presented in this paper), we compared the results of generic residue analysis and BV methods (S. Haaland, private communication, 2013). The BV method seems consistent with other single-spacecraft results like generic residue analysis methods [*Sonnerup et al.*, 2006]. For 3 March MVAB gives (0.99, 0.16, 0.01), MFR gives (0.96, 0.22, −0.17), MVAV gives (0.96, 0.23, −0.17), and COM gives (0.95, 0.24, −0.17), as BV finds (0.99, 0.05, 0.03). For 15 April, the same methods give, respectively, (0.99, −0.03, −0.11), (.96, −0.03, 0.27), (0.96, −0.07, 0.27), and (0.96, −0.10, 0.27), as BV gives (0.98, −0.18, −0.10). On "real" cases, one does not of course know the real normal direction, but we can observe that BV result is close to the generic residue Analysis methods results.

4. Products of the Method

As explained above, the first main direct product of the method is an accurate determination of the direction normal to the boundary, leading to reliable values of the small components B_n and u_n of the magnetic field and the flow velocity across the boundary. The second direct product is the determination of a spatial coordinate $y(t)$ allowing to draw any plasma parameter profile against the spatial position y from their temporal measurement. The magnetopause layer thickness is also an interesting by-product deriving directly from the two preceding ones.

Examples of y profiles are presented in Figure 11 for the crossing of 3 March 2008. Here we see the characteristic jump of density at the magnetopause, but no temperature jump, the pressure evolving like the density. For the different crossings that we investigated, we could often observe clear differences concerning the locations of the gradients of the plasma parameters (density, velocity, and pressure), with respect to the magnetic field rotation. In a companion paper [*Dorville et al.*, 2014], we present an interesting case study where the BV method helps obtaining new information about the nature of the magnetopause.

In Figure 12 the normal electric field obtained with the electric field and wave (EFW) experiment [*Gustafsson et al.*, 2001], and the tangential components are shown for the same 3 March 2008 crossing. We see that the maximum variance is on the normal electric field, as expected by theory, and quite constant tangential electric fields, which confirms that the normal direction found is a good one. Figure 13 shows the profiles of magnetic field spectral power density obtained with the Spatio-Temporal Analysis of Field Fluctuations (STAFF) experiment [*Cornilleau-Wehrlin et al.*, 2003] for different frequency ranges. One can observe that the source of waves lies in the magnetosheath and that the depth of penetration depends on the frequency, the lowest frequencies penetrating deeper toward the magnetospheric side.

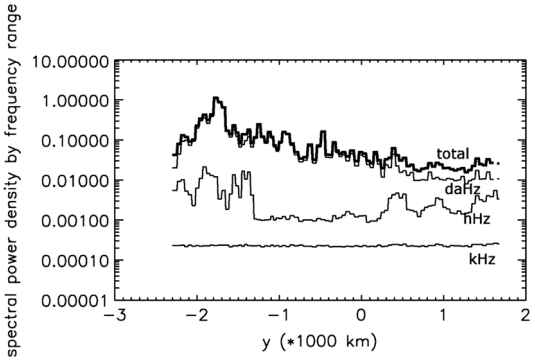

Figure 13. Evolution with normal position of the spectral power density (in nT^2) for magnetic field measured by Cluster C3 STAFF instrument. The total spectral power density is the thick line, as the daHz, hHz, and kHz frequency ranges are also represented on the same scale.

This ability to get spatial profiles of all the quantities in the boundary is a key to a better understanding of the physical nature of the magnetopause.

5. Discussion and Conclusion

We have presented the new BV method to analyze the structure of the magnetopause boundary layer, using spacecraft data. It combines the magnetic field and velocity measurements of one single spacecraft and permits to find the normal direction and a spatial coordinate which is determined with a resolution (close to the magnetic field time resolution) good enough to draw profiles on scales smaller than the layer width. Using it, we are able to study the internal structure of the layer, for any of the physical quantities measured on board. The method works on simulation and artificial data, and its assumptions can be verified on Cluster crossings.

It is worth observing the conditions of validity of the BV method are not the same as the other single-spacecraft methods such as MVAB, and that they are in general less restrictive. In MVAB, one needs to discriminate B_N and B_M, which fails systematically in structures such as shocks, and often at the magnetopause since this one is often quasi-coplanar (the maximum variance of the electric field is then more suitable). MVABC has the same condition of validity, with the additional problem that it cannot be used for determining B_n since this component is supposed to be null. In the BV method, one needs to discriminate the two couples of data sets: (B_N, V_N) and (B_M, V_M). This is clearly a weaker condition since, even if B_N and B_M are nearly constant, the differences between V_N and V_M, (profiles and/or orders of magnitude) are generally sufficient to guarantee a correct operation. The difficulties can only arise when not only B_N and B_M are indistinguishable (mean jump much smaller than noise) but also V_N and V_M.

Contrary to the multispacecraft timing methods, the BV method can also handle cases when the boundary is shaken with a nontrivial normal velocity evolution (which seems frequent). When this evolution is noticeable between the crossing times of the different spacecrafts, the timing methods or methods that assume a constant velocity or acceleration obviously fail.

The BV method however has it own and new limitations: although one works essentially with magnetic field data, a sufficiently long crossing is needed (at least three or four velocity measurement points inside the crossing) to make efficient the contribution of the velocity data. One will therefore not be able to use the method to analyze as many crossings as with the other methods. This makes the BV method difficult to compare with most of the existing benchmark cases or lists, since these ones are usually chosen to be well studied by timing methods. Forthcoming work will consist in performing statistics on a sufficiently large number of events to compare BV and other single-spacecraft methods. The domains of validity of the BV method and these methods are actually quite different. The BV method is certainly better suited to understand slow or long magnetopause crossings, while the usual methods would better work on short crossings. In the case of large B_n, it must be remembered anyway that the BV method cannot be used without special caution. It must also be noted that the normal determination, and so the spatial profiles, depends on the assumptions on the shape of the magnetic field hodogram and the evolution of the polar angle with position. A generalization is in preparation.

With the proposed method, the structure of the magnetopause should be now open to more detailed investigations. Some examples of spatial profiles have been given in section 4. The method is used in a companion article, for an atypical magnetopause case study giving new insight on this structure.

Acknowledgments

The authors would like to thank N. Cornilleau-Wehrlin for fruitful discussion and her help to work with Cluster data and detect magnetopause crossings, S. Haaland for his help with the GRA methods, and the CAA and all Cluster instruments teams for their work on Cluster data.

Philippa Browning thanks Johan De Keyser and two anonymous reviewers for their assistance in evaluating this paper.

References

Aunai, N., et al. (2013), Comparison between hybrid and fully kinetic models of asymmetric magnetic reconnection: Coplanar and guide field configurations, *Phys. Plasmas*, *20*, 022902.

Balogh, A., et al. (1997), The Cluster magnetic field investigation, *Space Sci. Rev.*, *79*(1-2), 65–91.

Belmont, G., N. Aunai, and R. Smets (2012), Kinetic equilibrium for an asymmetric tangential layer, *Phys. Plasmas*, *19*(2), 022108.

Cornilleau-Wehrlin, N., et al. (2003), First results obtained by the Cluster STAFF experiment, *Ann. Geophys.*, *21*, 437–456, doi:10.5194/angeo-21-437-2003.

De Keyser, J. (2006), The Earth magnetopause: Reconstruction of motion and structure, *Space Sci. Rev.*, *121*, 225–235.

De Keyser, J., and M. Roth (1998), Equilibrium conditions and magnetic field rotation at the tangential discontinuity magnetopause, *J. Geophys. Res.*, *103*(A4), 6653–6662, doi:10.1029/97JA03710.

Dorville, N., G. Belmont, L. Rezeau, R. Grappin, and A. Retinò (2014), Rotational/ Compressional nature of the Magnetopause: Application of the BV technique on a magnetopause case study, *J. Geophys. Res. Space Physics*, doi:10.1002/2013JA018927.

Dunlop, M. W., A. Balogh, K.-H. Glassmeier, and P. Robert (2002a), Four-point Cluster application of magnetic field analysis tools: The Curlometer, *J. Geophys. Res.*, *107*(A11), 1384, doi:10.1029/2001JA005088.

Dunlop, M. W., A. Balogh, and K.-H. Glassmeier (2002b), Four-point Cluster application of magnetic field analysis tools: The discontinuity analyzer, *J. Geophys. Res.*, *107*(A11), 1385, doi:10.1029/2001JA005089.

Gustafsson, G., et al. (2001), First results of electric field and density observations by Cluster EFW based on initial months of operation, *Ann. Geophys.*, *19*, 1219–1240, doi:10.5194/angeo-19-1219-2001.

Haaland, S., et al. (2004), Four-spacecraft determination of magnetopause orientation, motion and thickness: Comparison with results from single-spacecraft methods, *Ann. Geophys.*, *22*, 1347–1365.

Hasegawa, H. (2012), Structure and dynamics of the magnetopause and its boundary layers, *Monogr. Environ. Earth Planets*, *1*, 71–119, doi:10.5047/meep.2012.00102.0071.

Hasegawa, H., et al. (2004), Reconstruction of two-dimensional magnetopause structures from Cluster observations: Verification of method, *Ann. Geophys.*, *22*, 1251–1266.

Lockwood, M., and M. A. Hapgood (1997), How the magnetopause transition parameter works, *Geophys. Res. Lett.*, *24*, 373–376.

Mozer, F. S., and A. Retinò (2007), Quantitative estimates of magnetic field reconnection properties from electric and magnetic field measurements, *J. Geophys. Res.*, *112*, A10206, doi:10.1029/2007JA012406.

Panov, E. V., A. V. Artemyev, R. Nakamura, and W. Baumjohann (2011), Two types of tangential magnetopause current sheets: Cluster observations and theory, *J. Geophys. Res.*, *116*, A12204, doi:10.1029/2011JA016860.

Paschmann, G., and P. W. Daly (1998), *Analysis Methods for Multi-Spacecraft Data, No. SR-001 in ISSI Scientific Reports*, ESA Publ. Div., Noordwijk, Netherlands.

Paschmann, G., and B. U. Sonnerup (2008), Proper frame determination and Walén test, in *Multi-Spacecraft Analysis Methods Revisited*, edited by G. Paschmann and P. W. Daly, no. SR-008 in ISSI Scientific Reports, ESA Publ. Div., Noordwijk, Netherlands.

Powell, M. J. D. (1964), An efficient method for finding the minimum of a function of several variables without calculating derivatives, *Comput. J.*, *7*(2), 155–162, doi:10.1093/comjnl/7.2.155.

Rème, H., et al. (1997), The Cluster Ion Sectrometry (IS) experiment, *Space Sci. Rev.*, *79*, 303–350.

Russell, C. T., M. M. Mellot, E. J. Smith, and J. H. King (1983), Multiple spacecraft observations of interplanetary shocks: Four spacecraft determination of shock normals, *J. Geophys. Res.*, *88*, 4739–4748.

Sonnerup, B. U. O., and M. Scheible (1998), Minimum and maximum variance analysis, in *Analysis Methods for Multispacecraft Data*, edited by G. Paschmann and P. W. Daly, chap. 8, pp. 187–196, no. SR-001 in ISSI Scientific Reports, ESA Publ. Div., Noordwijk, Netherlands.

Sonnerup, B. U. O., S. Haaland, G. Paschmann, M. W. Dunlop, H. Rème, and A. Balogh (2006), Orientation and motion of a plasma discontinuity from single-spacecraft measurements: Generic residue analysis of Cluster data, *J. Geophys. Res.*, *111*, A05203, doi:10.1029/2005JA011538.

Soucek, J., and C. P. Escoubet (2012), Predictive model of magnetosheath plasma flow and its validation against Cluster and THEMIS data, *Ann. Geophys.*, *30*, 973–982, doi:10.5194/angeo-30-973-2012.